Surface Anisotropy and Spin-Reorientation Transitions in Ultrathin Magnetic Films

doi: 10.1109/20.539080

Surface Anisotropy and Spin-Reorientation Transitions in Ultrathin Magnetic Films

Xiao Hu
National Institute of Standards and Technology, Boulder, Colorado 80303, USA
and
Institute for Materials Research, Tohoku University, Sendai 980-77, Japan

Yoshiyuki Kawazoe
Institute for Materials Research, Tohoku University, Sendai 980-77, Japan

Abstract—**A micromagnetic theory is presented for spin-reorientation transitions in ultrathin magnetic films with normal surface anisotropy. Both discrete and continuum models are investigated and coincidence is found between the results derived from them. Two continuous transitions in spin orientation, from uniform and normal to canting, and then to uniform and in-plane, are observed as the film thickness is increased. The effects of higher-order terms in the expansions of the anisotropies compared to the dominant terms are also considered. A method for evaluating the surface anisotropy is formulated. The relation between the present micromagnetic theory and the phenomenological theory is discussed.**

I. Introduction

The stable configuration of magnetization in an ultrathin magnetic film coated by other materials, such as a Co film sandwiched by Au, changes with the film thickness: At lower thicknesses the magnetization is normal, and at higher thicknesses it is parallel, to the film plane. The in-plane magnetization configuration is favored by the shape anisotropy from dipolar interactions in the thin-film geometry, and thus is well understood. The normal magnetization is achieved by a strong normal anisotropy localized at the surface of the magnetic film. The existence of a surface anisotropy in magnetic films coated by other materials was first discussed theoretically by Néel [1] based on the breaking of translational symmetry at the surface. Experimental evidence for the normal surface anisotropy was obtained by Gradmann and Müller over two decades ago [2]. Since the normal magnetization state can be used for high-density magnetic and magneto-optic recording [3], the surface anisotropy is of considerable interests, both from the academic and applied points of view [4]–[9]. Spin-reorientation transitions are observed as the temperature is varied [10]–[15].

Spin reorientations in ultrathin magnetic films occur as the result of competition between the two above-mentioned anisotropies via ferromagnetic exchange coupling among neighboring atomic layers. Therefore, a micromagnetic approach is well suited for modeling and understanding this phenomenon [16]–[20].

Manuscript received March 3, 1996.

Present address of Xiao Hu: National Research Institute for Metals, 1-2-1 Sengen, Tsukuba 305, Japan; e-mail: xhu@nrim.go.jp

II. Discrete Model for Spin-Reorientation Transitions

Since spin-reorientation transitions have been observed in magnetic films of several atomic layers, the discreteness of these systems in the direction of the film normal must be considered by a theoretical treatment. We start by studying the following free energy functional [18],

$$\gamma = -Jm_s^2 \sum_{i=1}^{N-1} \cos(\varphi_i - \varphi_{i+1}) - K_v' \sum_{i=2}^{N-1} \sin^2 \varphi_i + K_s'(\sin^2 \varphi_1 + \sin^2 \varphi_N). \quad (1)$$

The first term covers the exchange coupling between the magnetization of adjacent atomic layers, where J is the exchange constant, m_s is the magnetization, and the orientation of magnetization φ is measured from the direction of the film normal. The second and third terms are for the volume anisotropy K_v' and the surface anisotropy K_s'. In the volume anisotropy term, the shape anisotropy part is assumed to dominate over the intrinsic part and thus $K_v' > 0$. In the above free energy functional, we have neglected domain structures across the film [20], [21], since we want to concentrate on the nonuniformity in the normal direction. This approximation is sufficient for many cases, noticing the difference between the size of domains across the film, of order of one micrometer, and the film thickness, of order of one nanometer [6]. It is also assumed that the demagnetization factor (involved in K_v'), the surface anisotropy, and the magnetization are independent of the film thickness, an assumption not always accurate, true [4].

We have calculated the stable magnetic configuration using the variational technique. Fixing the magnetic constants, we have found a spin-reorientation transition from a uniform and normal configuration to a canting configuration as the number of layers N is increased. Another transition is observed when N is increased further, where the canting configuration is converted into a uniform and

0018-9464/96$05.00 © 1996 IEEE

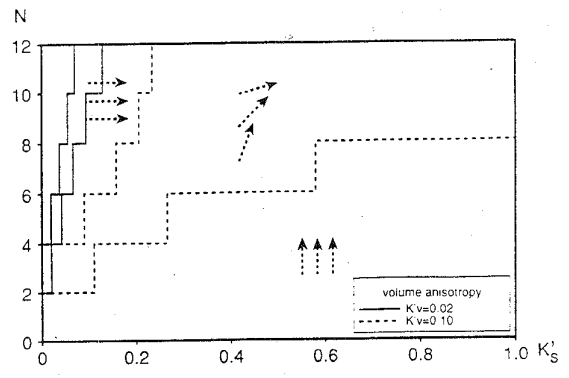

Fig. 1. Phase diagram with the number of atomic layers and the surface anisotropy as variables. The magnetic anisotropies are normalized in unit of $\frac{1}{2}Jm_s^2$. The typical configuration in each phase for $K_v' = 0.1$ is denoted by the dashed arrows.

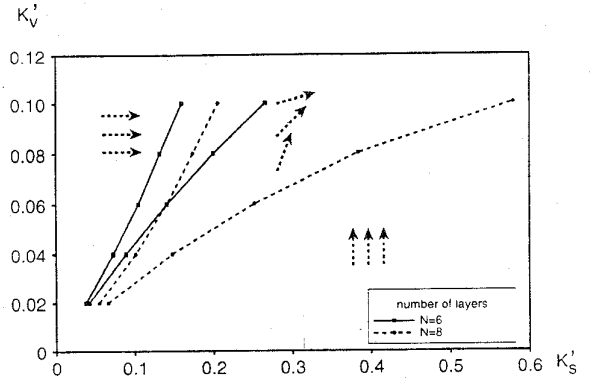

Fig. 2. Phase diagram with the shape anisotropy and the surface anisotropy as variables. The magnetic anisotropies are normalized in unit of $\frac{1}{2}Jm_s^2$. The typical configuration in each phase for $N = 8$ is denoted by the dashed arrows.

in-plane configuration. The phase diagram with the number of atomic layers and the surface anisotropy as variables is depicted in Fig. 1, for two different values of volume anisotropy, where the magnetic anisotropies are normalized in unit of $\frac{1}{2}Jm_s^2$. The phase boundaries consist of steps, as the result of the discrete variation of the thickness, namely the number of atomic layers. The locations of the phase boundaries depend sensitively on the value of volume anisotropy. The two phase boundaries shift towards the N axis when K_v' decreases. The canting phase exists in a very small region, as seen from Fig. 1. This explains why it is difficult to observe the canting structure experimentally.

We have also investigated the stable configuration for different values of the volume anisotropy and the surface anisotropy in magnetic films of fixed thickness. This situation can be realized by experimental observations on a given sample at different temperatures. The phase diagram thus obtained is given in Fig. 2. We find three phases, similarly to those in Fig. 1. The locations of the phase boundaries depend sensitively on the number of atomic layers. Similarity is found between the two phase diagrams in Figs. 1 and 2. The physical origin of this similarity is as follows: Increasing the value of K_v' enhances the force to align the magnetization into the film plane *intensively*, while the increase of the number of atomic layers enhances this force *extensively*, since the surface anisotropy is localized at the surface atomic layers.

This similarity is not only qualitative but can also be described quantitatively. To this end, we have calculated the magnetic configurations in systems with $N = 4$ to 20 and with various values of K_s' and K_v'. By using two renormalized variables, $(N - \Delta N)\sqrt{K_v'}$ and $K_s'/\sqrt{K_v'}$, and choosing $\Delta N = 2.2$, all the phase boundaries, such as those in Figs. 1 and 2, collapse into two smooth curves, as shown in Fig. 3. This indicates the presence of the scaling relations among the film thickness, the two anisotropies, and the exchange coupling in the spin-reorientation transitions: $(N - \Delta N)\sqrt{K_v'/(Jm_s^2)}$ and $K_s'/\sqrt{K_v' Jm_s^2}$.

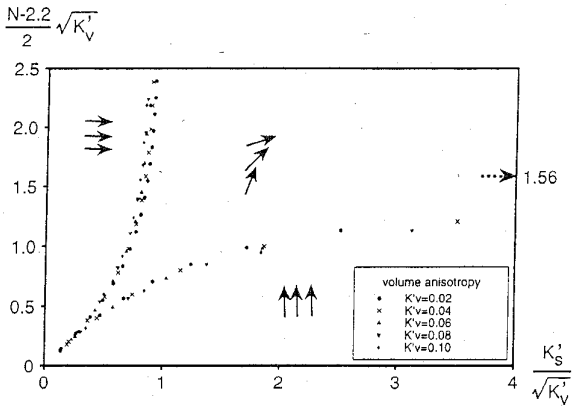

Fig. 3. Phase diagram with scaled variables. The magnetic anisotropies are normalized in unit of $\frac{1}{2}Jm_s^2$. The typical configuration in each phase is denoted by the arrows.

The scaling relations mentioned above are satisfied sufficiently in the whole region of surface anisotropy $K_s'/\sqrt{K_v' Jm_s^2}$, while only for small volume anisotropies:

$$K_v'/(Jm_s^2) \leq 0.04. \tag{2}$$

For transition metals like Fe, however, K_v' is about $0.003Jm_s^2$ [18]. Therefore, we expect the scaling behaviors shown in Fig. 3 should be observed experimentally. Meanwhile, this scaling plot provides a unified way to analyze experimental data on spin-reorientation transitions observed in different materials. It may be used for plotting data at different temperatures within the region where the magnetic quantities vary with temperature while fluctuation effects are not critical.

We notice two features of the phase diagram in Fig. 3: First, the phase boundary between the canting phase and the uniform and in-plane phase diverges at unity; Second, the phase boundary between the canting phase and

the uniform and normal phase saturates at about 1.65. We shall explain these two features by the results of the continuum model in the next section. The meaning of $\Delta N \simeq 2.2$ will also be discussed.

III. Continuum Model for Spin-Reorientation Transitions

In order to understand the numerical results in the preceding section, we show results of the continuum model [16], [17]. Continuum models have been used for the study of the magnetic structures in semi-infinite systems with surface anisotropy by several authors [22]–[24]. Consider a thin magnetic film of thickness $2a$: On the surfaces there exist normal anisotropies K_s; within the film the shape anisotropy K_v is in the film plane; and the exchange stiffness A is ferromagnetic and finite. From the symmetry of the system, we consider only half of the system. The free energy functional is

$$\gamma = \int_0^a \left[A(\frac{d\varphi}{dz})^2 - K_v \sin^2 \varphi \right] dz + K_s \sin^2 \varphi(0), \quad (3)$$

where the z axis is taken to be normal to the film plane and the origin at the bottom surface. The relations among the magnetic quantities in functionals (1) and (3) are given by: $JM_s^2 \hat{a}/2 = A$, $K_v'/\hat{a} = K_v$ and $K_s' = K_s$, where $\hat{a}$ is the lattice constant.

The stable magnetization configuration is determined by solving the variational problem for energy functional (3). The Euler equation is

$$2A\frac{d^2\varphi}{dz^2} + K_v \frac{d\sin^2\varphi}{d\varphi} = 0 \quad (4)$$

with two boundary conditions

$$\begin{cases} \dfrac{d\varphi}{dz}|_{z=a} = 0, \\ A\dfrac{d\varphi}{dz}|_{z=0} = K_s \sin\varphi(0)\cos\varphi(0). \end{cases} \quad (5)$$

There are two trivial solutions to the above differential equation and the boundary conditions, $\varphi = 0$ or π and $\varphi = \pi/2$.

The problem of solving the differential equation (4) under the conditions (5) is reduced to the problem of solving the following nonlinear equation for the orientation of magnetization at $z = a$ [17]

$$\frac{K_s}{\sqrt{AK_v}} = \frac{\mathrm{sn}[a\sqrt{K_v/A}, \sin\varphi_a]\mathrm{dn}[a\sqrt{K_v/A}, \sin\varphi_a]}{\mathrm{cn}[a\sqrt{K_v/A}, \sin\varphi_a]}, \quad (6)$$

with $\varphi_a \equiv \varphi(a)$. The Jacobi elliptic functions $\mathrm{sn}[x,k]$, $\mathrm{cn}[x,k]$, and $\mathrm{dn}[x,k]$ involved in the above equation are defined by

$$u = \int_0^{\sin^{-1}(\mathrm{sn}[u,k])} \frac{d\theta}{\sqrt{1-k^2\sin^2\theta}} \quad (7)$$

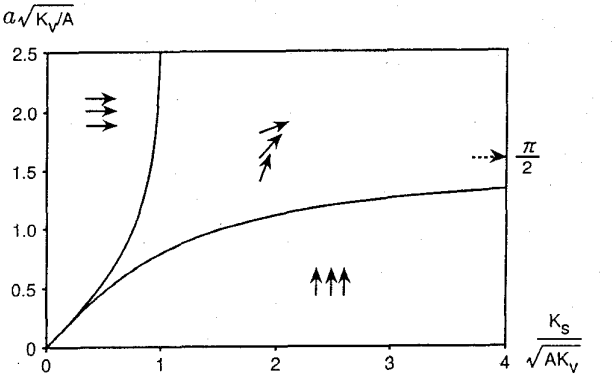

Fig. 4. Phase diagram obtained by the continuum model. The typical configuration in each phase is denoted by the arrows.

and the relations $\mathrm{sn}^2[x,k] + \mathrm{cn}^2[x,k] = 1$ and $k^2\mathrm{sn}^2[x,k] + \mathrm{dn}^2[x,k] = 1$. The magnetization configuration for $0 \le z \le a$ is expressed by φ_a as

$$\varphi(z) = \sin^{-1}\left\{ \sin\varphi_a \frac{\mathrm{cn}[(a-z)\sqrt{K_v/A}, \sin\varphi_a]}{\mathrm{dn}[(a-z)\sqrt{K_v/A}, \sin\varphi_a]} \right\}. \quad (8)$$

The phase boundary between the canting configuration phase and uniform and normal configuration phase is derived by putting $\varphi_a = 0$ in (6) and using the relations $\mathrm{sn}[u,0] = \sin u$, $\mathrm{cn}[u,0] = \cos u$, and $\mathrm{dn}[u,0] = 1$:

$$a_{c1} = \sqrt{A/K_v}\tan^{-1}(K_s/\sqrt{AK_v}). \quad (9)$$

The phase boundary between the phase of canting configuration and the phase of uniform and in-plane configuration is derived by putting $\varphi_a = \pi/2$ in (6) and using the relations $\mathrm{sn}[u,1] = \tanh u$ and $\mathrm{cn}[u,1] = \mathrm{dn}[u,1]$:

$$a_{c2} = \sqrt{A/K_v}\tanh^{-1}(K_s/\sqrt{AK_v}). \quad (10)$$

The phase diagram is given in Fig. 4. We find good agreement between the scaled phase diagram Fig. 3 from the discrete model and the phase diagram Fig. 4 from the continuum model. From the two functions in (9) and (10), the phase boundary between the uniform and normal phase and the canting phase should saturate at $a\sqrt{K_v/A} = \pi/2$ as indicated by the dashed arrow in Fig. 4, and the phase boundary between the uniform and in-plane phase and the canting phase should diverge at $K_s/\sqrt{AK_v} = 1$. Therefore, the numerical results in the preceding section are explained by the analytical expressions derived from the continuum model.

The coincidence between the scaled phase diagram obtained from the discrete model and the phase diagram obtained from the continuum model justifies the use of the continuum approach in the study of magnetic properties of ultrathin magnetic films of several atomic layers.

We can see this point in the following, alternative way. Condition (2) can be rewritten in terms of the magnetic

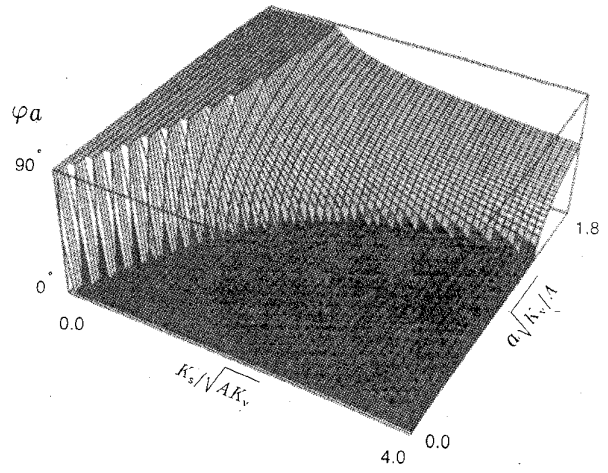

Fig. 5. Thickness and surface-anisotropy dependences of the orientation of magnetization at the film center.

quantities of the continuum model and the lattice spacing as

$$\hat{a} \leq 0.28\sqrt{A/K_v}, \tag{11}$$

namely, the lattice spacing should be much smaller than the domain-wall width $\sqrt{A/K_v}$. Therefore, the condition for the accuracy of the continuum model is equivalent to the criterion for scaling of the results obtained from the discrete model, which is satisfied by the transition metals as shown in the preceding section.

From Figs. 3 and 4, the film thickness in the continuum model should be evaluated from the number of atomic layers of the relevant lattice as

$$a = (N - \Delta N)\hat{a}, \tag{12}$$

with $\Delta N \simeq 2$. The physical meaning of ΔN becomes clear when comparing the two treatments of surface anisotropy in (1) and (3). In other words, the treatment of surface anisotropy in the continuum model (3) is correct only when the film thickness is evaluated as in (12).

Let us see in more detail the physical content of the results from the continuum model. We find in (9) and (10) that $\sqrt{A/K_v}$, the domain-wall thickness in a bulk system, is also the characteristic length in describing spin-reorientation transitions in ultrathin films. However, there is the factor $\tan^{-1}(K_s/\sqrt{AK_v})$ in (9) and the factor $\tanh^{-1}(K_s/\sqrt{AK_v})$ in (10). When the ratio $K_s/\sqrt{AK_v}$ is very small, which is the case for many magnetic materials, they are approximately equal to $K_s/\sqrt{AK_v}$. These two factors make spin reorientations occur in magnetic films of ultra small thicknesses, sometimes of only a few atomic layers, which are much smaller than $\sqrt{A/K_v}$.

The thickness and surface-anisotropy dependences of the orientation of magnetization at $z = a$, the center of magnetic film, is summarized in Fig. 5. Fig. 6 shows the thickness dependence of magnetization orientations

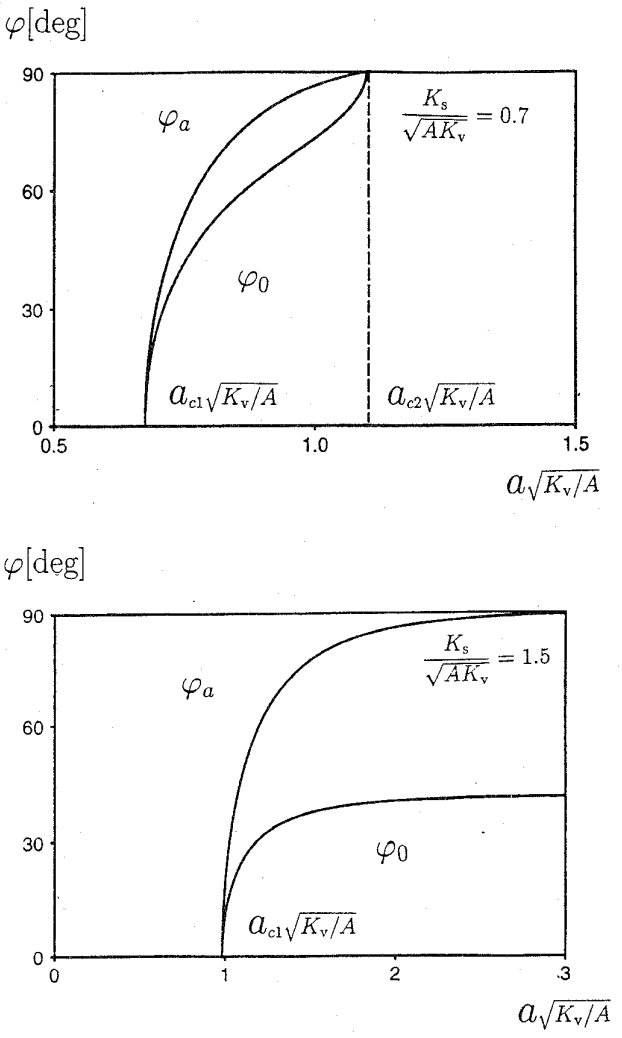

Fig. 6. Thickness dependence of the orientation of magnetization at the film center and that on the surface for $K_s/\sqrt{AK_v} < 1$ (top) and for $K_s/\sqrt{AK_v} > 1$ (bottom).

φ_a and $\varphi(0)$. For $K_s/\sqrt{AK_v} \leq 1$, both φ_a and $\varphi(0)$ saturate to $\pi/2$ at $a = a_{c2}$. We find a direct correspondence between this theoretical result shown in the top graph in Fig. 6 with the experimental observation in [6]. For $K_s/\sqrt{AK_v} > 1$, however, $\varphi(0)$ assumes an intermediate orientation even at the large-thickness limit where φ_a saturates at $\pi/2$. The saturation value of $\varphi(0)$ is derived from (6) and (8) as

$$\lim_{a\to\infty} \varphi(0) = \sin^{-1}(\sqrt{AK_v}/K_s). \tag{13}$$

IV. Discussion about the Phenomenological Theory

In the phenomenological theory for spin-reorientation transitions, the free energy is approximated by

$$\gamma = -K_v a + K_s. \tag{14}$$

Spin-reorientation transitions are attributed to the balance between the normal surface anisotropy and the in-plane shape anisotropy. The critical thickness is derived by setting $\gamma = 0$ in (14):

$$a_c = K_s/K_v. \tag{15}$$

Below a_c, the magnetization is uniform and normal to the film plane; above a_c, the magnetization is uniform and parallel to the film plane. The transition between these two states is discrete.

At the limit of small surface anisotropy and/or large exchange stiffness, (9) and (10) collapse into (15). The phenomenological theory thus seems consistent with the present micromagnetic theory for $K_s/\sqrt{AK_v} \ll 1$. However, in the micromagnetic theory the linear thickness dependence of free energy (14) applies only for $K_s/\sqrt{AK_v} < 1$ and $a > a_{c2}$, where the uniform and in-plane configuration is stable. Since

$$a_{c1} < a_c < a_{c2}, \tag{16}$$

the balance between the two anisotropies never happens in the micromagnetic point of view. In this sense, the mechanism suggested by the phenomenological theory is misleading.

In the transient phase derived from the micromagnetic theory, the normal surface anisotropy dominates over the in-plane shape anisotropy near the surface, and vice versa at the center part of the film. Therefore, during the transition between the normal magnetization state and the in-plane magnetization state, these two anisotropies sustain magnetic long-range orderings with different orientations in the two parts of the film. This resolves the puzzle: The cancelation between the two anisotropies triggers spin-reorientation transitions, while no long-range ordering is possible at all with zero anisotropy in ultrathin films of effectively two dimensions, from the Mermin-Wagner theorem [25].

For $K_s/\sqrt{AK_v} > 1$, the canting configuration remains stable even at the large-thickness limit. The constant term in the free energy asymptote becomes more complex. At large thickness, where $\varphi_a \to \pi/2$,

$$A(d\varphi/dz)^2 = K_v(\sin^2\varphi_a - \sin^2\varphi) \simeq K_v\cos^2\varphi \tag{17}$$

from (4) and (5). Therefore, we have the following asymptote of the free energy [17]:

$$\gamma \simeq -K_v a + 2\sqrt{AK_v} - AK_v/K_s, \tag{18}$$

where (13) is included in the last step. The constant term in the above asymptote can be called the surface energy, which is shown analytically to be smaller than the surface anisotropy K_s. The large surface-anisotropy energy relaxes into the canting structure.

The canting structure near the surface should affect the resonating field of a ferromagnetic resonance (FMR) measurement. Not only the surface anisotropy K_s, as in (14), but also the exchange stiffness A and the shape anisotropy K_v are involved in the thickness dependence of the resonating field, as in (18). This point has been mentioned in [26].

V. Higher-Order Anisotropies

In many materials, higher-order terms in the expansions of the anisotropies are of comparable magnitudes with the dominant terms included in free energy functional (3), and thus should also be taken into account. In this paper we show briefly some results including the biquadratic anisotropies. The free energy functional is given as

$$\gamma = \int_0^a \left[A(\frac{d\varphi}{dz})^2 - K_{v1}\sin^2\varphi - K_{v2}\sin^4\varphi\right] dz + K_{s1}\sin^2\varphi(0) + K_{s2}\sin^4\varphi(0). \tag{19}$$

The critical thickness between the uniform and normal phase and the canting phase is given by

$$a_{c1} = \sqrt{A/K_{v1}}\tan^{-1}(K_{s1}/\sqrt{AK_{v1}}). \tag{20}$$

The critical thickness between the uniform and in-plane phase and the canting phase is

$$a_{c2} = \sqrt{\frac{A}{K_{v1}+2K_{v2}}}\tanh^{-1}\frac{K_{s1}+2K_{s2}}{\sqrt{A(K_{v1}+2K_{v2})}}. \tag{21}$$

Both of these two expressions are similar to their counterparts in section III. Therefore, the model that includes only the dominant anisotropy terms can explain most of the properties of spin-reorientation transitions. However, the model including higher order anisotropies predicts more complex classification of spin-reorientation transitions [8] since the case $a_{c1} > a_{c2}$ is possible, in principle.

VI. Method for Measuring the Surface Anisotropy

It is important to measure the surface anisotropy to high accuracy. One way to do this is using FMR technique. Next we formulate a method which can be used with magneto-optical Kerr effect (MOKE) [27] or spin scanning electron microscopy with polarization analysis (SEMPA) measurements [28].

By means of the first relation in (17), we evaluate the total z component of magnetization when the system assumes a canting configuration:

$$M_z = 2\int_0^a m_s\cos\varphi dz = 2m_s\sqrt{\frac{A}{K_v}}\cos^{-1}\left[\frac{\sin\varphi(0)}{\sin\varphi_a}\right]. \tag{22}$$

As the ratio $\sin\varphi(0)/\sin\varphi_a$ can be expressed by φ_a with (8), we arrive at the following relation:

$$\frac{\mathrm{cn}[a\sqrt{K_v/A}, \sin\varphi_a]}{\mathrm{dn}[a\sqrt{K_v/A}, \sin\varphi_a]} = \cos\left[\frac{M_z}{2m_s\sqrt{A/K_v}}\right]. \quad (23)$$

Therefore, if an accurate measurement of the total z component of magnetization is available, we can determine φ_a by solving numerically the above nonlinear equation. The surface anisotropy is then evaluated by (6).

This method for evaluating the surface anisotropy can be applied to systems where the surface anisotropy depends on the film thickness and thus techniques involving thickness extrapolation are not applicable. The limitation of the present method is that it can be used only when the system is in the canting phase.

VII. Summary

Spin-reorientation transitions in ultrathin magnetic films with normal surface anisotropy are studied theoretically by means of the micromagnetic approach. Both discrete and continuum models are investigated. Scaling relations among the number of atomic layers, the surface anisotropy, the volume anisotropy, and the exchange stiffness are derived, which provide a unified way for analyzing experimental data for various materials at different temperatures. When the scaling variables are used, the phase diagram for the stable magnetization configuration derived from the discrete model coincides with that derived from the continuum model. The sufficiency of the continuum approach to spin-reorientation transitions occurring in ultrathin films of a few atomic layers is thus proved.

Two continuous transitions of spin orientation, from uniform and normal to canting, and then to uniform and in-plane, are observed as the film thickness is increased. Analytic expressions for the two critical thicknesses are presented. The reason why significant variations of spin orientation can be achieved with such a small change of film thickness of only a few atomic layers is discussed.

In the micromagnetic theory, balance between the normal surface anisotropy and the in-plane shape anisotropy does not happen during the transitions. On the other hand, in the phenomenological theory, the cancellation between these two anisotropies triggers spin-reorientation transitions, even though no long-range ordering is possible for zero anisotropy in ultrathin films.

The effects of higher-order anisotropies on the spin-reorientation transitions are discussed. A method for evaluating the surface anisotropy is formulated based on the micromagnetic calculation, which may be combined with MOKE or SEMPA measurements on the total normal component of magnetization.

Acknowledgment

Xiao Hu thanks R. B. Goldfarb for fruitful discussions and suggestions. He gratefully acknowledges the hospitality extended to him during his tenure as Guest Research Scientist at NIST-Boulder, where part of this work was done.

References

[1] L. Néel, *J. Phys. Rad.*, vol. 15, p. 376, 1954.
[2] U. Gradmann and J. Müller, *Phys. Stat. Sol.* , vol. 27, p. 313, 1968.
[3] J. Ferré, G. Pénissard, C. Marliere, D. Renard, P. Beanvillain, and J. P. Renard, *Appl. Phys. Lett.*, vol. 56, p. 1588, 1990.
[4] B. Heinrich, J. F. Cochran, A. S. Arrott, S. T. Purcell, k. B. Urquhart, J. R. Dutcher, and W. F. Egelhoff, Jr., *Appl.Phys.*, vol. A49, p. 473, 1989.
[5] C. Chappert and P. Bruno, *J. Appl. Phys.*, vol. 64, p. 5736, 1988.
[6] R. Allenspach, M. Stampanoni, and A. Bischof, *Phys. Rev. Lett.*, vol. 65, p. 3344, 1990.
[7] V. Grolier, J. Ferre, A. Maziewski, E. Stefanowicz, and D. Renard, *J. Appl. Phys.*, vol. 73, p. 5939, 1993.
[8] H. Fritzsche, J. Kohlhepp, H. J. Elmers, and U. Gradmann, *Phys. Rev. B*, vol. 49, p. 15665, 1994.
[9] I. Harada, O. Nagai, and T. Nagamiya, *Phys. Rev. B*, vol. 16, p. 4882, 1977.
[10] J. J. Krebs, B. T. Jonker, and G. A. Prinz: *J. Appl. Phys.* , vol. 63, p. 3467, 1988.
[11] M. Stampanoni, A. Vaterlaus, M. Aeschlimann, and F. Meier, *Phys. Rev. Lett.*, vol. 59, p. 2483, 1987.
[12] D. Pescia and V. L. Pokrovsky, *Phys. Rev. Lett.*, vol. 65, p. 2599, 1990.
[13] D. P. Pappas, K. P. Kamper, and H. Hopster: *Phys. Rev. Lett.*, vol. 64, p. 3179, 1990.
[14] A. Berger, A. W. Pang, and H. Hopster, *J. Magn. Magn. Mater.* , vol. 137, p. L1, 1994.
[15] S. D. Bader, D. Q. Li, and Z. Qui, *J. Appl. Phys.*, vol. 76, p. 6419, 1994.
[16] A. Thiaville and A. Fert, *J. Magn. Magn. Mater.* , vol. 113, p. 161, 1992.
[17] X. Hu and Y. Kawazoe, *Phys. Rev. B*, vol. 51, p. 311, 1995.
[18] X. Hu and Y. Kawazoe, "New estimation of surface anisotropy," *J. Appl. Phys.*, vol. 79, No. 8, 1996, in press.
[19] X. Hu, T. Yorozu, Y. Kawazoe, S. Ohnuki, and N. Ohta, *IEEE Trans. Magn.*, vol. 29, p. 3790, 1993; X. Hu and Y. Kawazoe, *Phys. Rev. B*, vol. 49, p. 3294, 1994; *ibid*, *J. Appl. Phys.*, vol. 75, p. 6486, 1994.
[20] R.-B. Tao, X. Hu, and Y. Kawazoe, *Phys. Rev. B*, vol. 52, p. 6178, 1995.
[21] Y. Yafet and E. M. Gyorgy, *Phys. Rev. B*, vol. 38, p. 9145, 1988.
[22] D. L. Mills, *Phys. Rev. B*, vol. 39, p. 12306, 1989.
[23] R. C. O'Handley and J. P. Woods, *Phys. Rev. B*, vol. 42, p. 6568, 1990.
[24] A. Aharoni, *Phys. Rev. B*, vol. 47, 8296, 1993.
[25] N. D. Mermin and H. Wagner, *Phys. Rev. Lett.*, vol. 17, p. 1133, 1966.
[26] G. T. Rado, *Phys. Rev. B*, vol. 26, p. 295, 1982.
[27] H. J. Elmers, G. Liu, H. Fritzsche, and U. Gradmann, *Phys. Rev. B*, vol. 52, p. R696, 1995.
[28] J. Unguris, R. J. Celotta, and D. T. Pierce, *J. Magn. Magn. Mater.* , vol. 127, p. 205, 1993; *ibid*, *Phys. Rev. Lett.*, vol. 69, p. 1125, 1992.